

# Cosmic Ray Muons: Detection and Analysis

Brian Riendeau, Supervisor: Dr. Lewis Riley

Fall 2022

## Contents

<b>1</b>	<b>Introduction</b>	<b>1</b>
1.1	Background . . . . .	1
1.2	Motivation . . . . .	2
<b>2</b>	<b>Experiment</b>	<b>2</b>
2.1	Methods . . . . .	2
<b>3</b>	<b>Analysis and Results</b>	<b>3</b>
3.1	Single Muon Coincidence Histogram . . . . .	3
3.2	Decay-time Spectrum . . . . .	3
3.3	Muon and Decay Pulse-Height Histograms . . . . .	4
<b>4</b>	<b>Discussion</b>	<b>4</b>
<b>5</b>	<b>Summary</b>	<b>5</b>

## Abstract

Using pulse-height analysis with a 3" x 3" cylindrical Sodium-Iodide (NaI) detector to look for cosmic ray muons, we analysed a time series of voltage signals over 671 hours to identify events in which two pulses were detected within 40  $\mu$ s. We analyzed these traces to measure the lifetimes and energy-loss spectra of these events. After 671 hours (3.99 weeks) of data collection, we successfully measured the lifetimes and energy properties of low-energy muon decays at Ursinus College. We measured the muon mean lifetime to be  $2.103 \pm 0.013 \mu$ s. In total, 5,552 potential muon decay events were detected which we then used to produce energy-loss spectra. We identified unique characteristics in the muon energy-loss spectra compared to the following decay particle spectra by observing their signal patterns.

## 1 Introduction

### 1.1 Background

Cosmic radiation incident at the top of the Earth's atmosphere consists of stable charged particles and nuclei with lifetimes on the order of  $10^6$  years or even longer [4]. We define primary cosmic rays as particles that come from astrophysical sources while secondary cosmic rays have their origins from interactions between primary cosmic rays and interstellar gas [4]. Approximately 79% of primary cosmic radiation is composed of free protons and about 70% of the remaining comes from the nucleons in helium nuclei [4].

Muons are secondary cosmic rays produced in a cosmic ray cascade event [3]. While the atoms and molecules in Earth's atmosphere are being continuously bombarded with cosmic rays, several newly formed particles are created in a cascade event as a result of these collisions [3]. A typical cascade event occurs when a proton strikes a molecule and produces pions, neutrinos, gamma rays, electrons, a neutron, and muons [3]. More specifically, muons and neutrinos are by-products of the decays of charged mesons [4]. Photons and electrons on the other-hand are by-products of the decays of neutral mesons [4]. These incident muons will travel towards the Earth moving at speeds approximately .99c (speed of light in vacuum) [1]. The muons will then decay themselves in approximately 2.2  $\mu$ s while at rest, which is the average lifetime for slowed muons approaching sea-level [4]. Depending on the muon's charge, they will decay into either an electron or positron, a neutrino, and an anti-neutrino [1].

The majority of primary cosmic radiation comes from outside the solar system while a small portion also comes from solar flares [4]. Incoming charged particles are changed through interactions with the solar wind; this process eliminates some of the low energy cosmic rays before they reach us by interactions with the magnetized plasma generated from the sun [4]. Lower-energy cosmic rays are also affected by the geomagnetic field; incoming radiation must pass through this field to reach the top of the Earth's atmosphere [4]. The intensity of the radiation in the GeV range will depend on both location and time [4]. We expect muons to be hitting our atmosphere and arriving at our detector at ground level with a mean energy of 4 GeV after losing about 2 GeV to ionization and radiative processes on its typical 15 km decay trajectory [4].

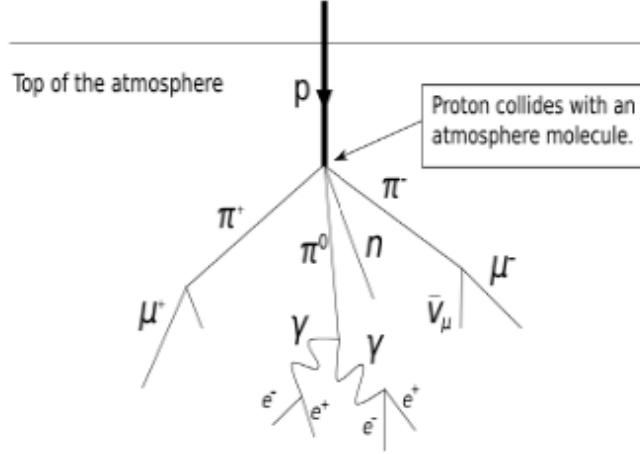


Figure 1: A typical cosmic-ray cascade event triggered by cosmic ray protons colliding with atmospheric molecules. Reprinted From: (The Decay of Muons by Sherman Ip)

## 1.2 Motivation

To understand how muons interact in our lab environment we use ground-based detectors to test for incident muons here at Ursinus. We expect to detect mostly  $\mu^+$  (antimuons) and their decay particle the positron using our NaI detector. The majority of negative muons are captured by atoms in the detector and therefore do not generate decay signals. The remaining atmospheric neutrino and antineutrino particles will not have an appreciable effect within our detector due to having small interaction cross sections [4]. Equation 1 shows the expected decay process for a muon captured in our detector [1]. While Equation 2 shows another commonly found decay arrangement.

$$\mu^+ \rightarrow e^+ + \nu_e + \bar{\nu}_\mu \quad (1)$$

$$\mu^- \rightarrow e^- + \nu_e + \bar{\nu}_\mu \quad (2)$$

## 2 Experiment

### 2.1 Methods

Our data acquisition system was a Pico-Scope digital oscilloscope. Using the associated signal tracking software coupled to our Sodium-Iodide (NaI) detector we performed a sequence of 671 consecutive hour long runs (approximately 4 weeks) to determine potential candidates for cosmic-ray muon decays [5]. We assumed the average muon would be approaching sea-level with 4 GeV of energy and would be vertically incident on our 3-inch width detector NaI crystal [4]. Muons that approach sea-level lose energy through ionization and radiative processes and therefore only a small fraction of muons reach our detector and produce the specific decay process we are looking to detect [4]. The surviving muons arrive at our detector with much lower energies (MeV) than the larger fraction which pass straight through without decaying. Due to these low-energy muons, we are able to slow them down enough to completely stop them. We therefore detected a selective portion of their constituent decay particles for incident muons with lower-energies.

These low-energy trace coincidences were measured using a single channel that was connected to a high-voltage input which served as input for the photo-multiplier tube (PMT). Integrated inside the PMT is a preamplifier that amplifies the signal. This amplified signal is what feeds our Pico-Scope device. The threshold voltage was set to exclude background x-ray events that would interfere with our data acquisition. Our sampling time window in seconds was set to  $1\text{ }\mu\text{s}$  pre-trigger and  $40\text{ }\mu\text{s}$  post-trigger. This window allows observation over the entire lifespan for an average muon stopped in the detector because the unstable muon has a mean lifetime of approximately  $2.2\text{ }\mu\text{s}$  [4]. The window is extended in duration to allow for the detection of background events due to accidental coincidences between muons passing through the detector. Measuring significant background signal provides further verification that our signal was accurately measuring expected muon decays. This process enabled us to establish a baseline voltage measurement which was needed to extract out the relevant incoming muon energy deposits.

### 3 Analysis and Results

In order to determine the maximum pulse-heights for both muons and their decays, we applied a gradient function to the voltage readings then selected maximum rates of change: equating to the start locations for both voltage signals. Using pulse-height spectrum analysis we collected sets of data, specifically, three separate arrays to store the decay times, muon-pulse-heights, and decay-pulse-heights. We also created a corresponding set of arrays to monitor the time and voltage for each hour long run interval in our 671 hour sample set in order to cross-correlate events. By applying gradient analysis over the voltages we were also able to determine the starting and ending voltages for muon-decay processes.

A potential decay event was determined to be a valid candidate if the secondary peak in voltage was within a short window after the first peak was detected. A peak finding algorithm was then applied by using the gradient of the voltages. We manual adjusted the width to match the range of signal variations using an estimation of the cross-references in the time and gradient spike positions. We calculated a baseline voltage by averaging over a 10 point interval before the pulse-signal rise. After obtaining our maximum voltages at the first and second peak locations we were able to subtract the baseline voltages and obtain our two pulse height values that occurred in our  $40\text{ }\mu\text{s}$  post-trigger window. The decay time was obtained by taking the time differences between the first and second pulses.

#### 3.1 Single Muon Coincidence Histogram

Using our detector we measured the energy spectra of single muon events from our 671 hour data set shown in figure 2. From our single muon event data, we observed a large number of low-energy muons detected above our threshold. We used this graph to calibrate our energy spectra for the muon-decay events. Figure 2 demonstrates the high energy-loss cutoff which was set high enough to record the vast majority of events. The starting high-end position from figure 2 records all muons while the gap below this value equates to the exclusion of gamma rays below our threshold. From the total data set (671 hours), we recorded 5,552 potential muon-decay events. If this experiment were to be ran in a week-long trial that could be used for future class experiments, our results from 7 days (168 hours) of data indicate a potential of 1,368 decay events. A similar analysis on week long data should produce results consistent with our energy spectra although with higher uncertainties due to lower numbers of total counts being measured.

#### 3.2 Decay-time Spectrum

With our muon and decay pulse-heights established we then generated a lifetime measurement signal distribution. Our model shown in figure 3, is our original resulting dual-coincidence pulse height decay spectrum plotted with an exponential fit. On the vertical axis we have counts per microsecond from the moment of trigger occurrence to  $40\text{ }\mu\text{s}$ . Included within this data is the background counts where no alterations to the signal were used. Therefore the results are in agreement with exponential decay. Error bars fitted to the original data use the square root of the counts. We conclude that for the expected  $2.2\text{ }\mu\text{s}$  decay period a high degree of accuracy was maintained in detecting a muon decay event into positrons. Electrons decays are not typically detected with our detector due to being captured by atoms. This discrepancy can be accounted for with our optimized decay time of  $2.103\text{ }\mu\text{s} \pm 0.013$ .

From figure 3 we account for deviations from the exponential fit in our original data by using the background estimate over the  $40\text{ }\mu\text{s}$  event window which reported a singles rate of  $R_s = 1.306\text{ }\mu/\text{s}$ . We used this singles rate to find the probability per decay event  $P(double) = R_s \Delta t = 40\text{ }\mu\text{s} * 1.306 = 5.224 * 10^{-5}$ .

Using this probability we calculated the number of events above  $20\text{ }\mu\text{s}$  which come from accident muon coincidences using the total number of triggers  $N_t = 3152474$  and  $P(double)$ . Thus,  $N_t * P(double) = 165$  or  $\frac{4\text{ counts}}{\text{bin}}$ .

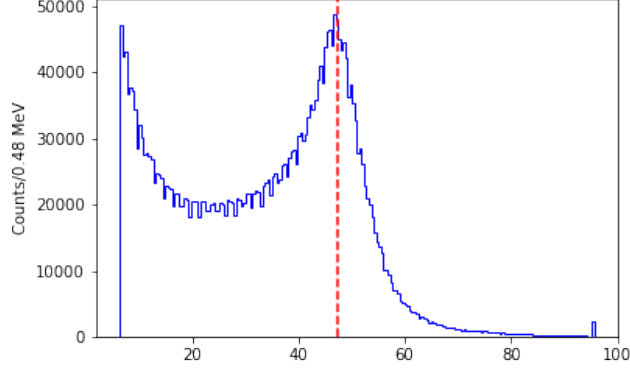


Figure 2: Single muon events spectrum with our calibrated energy loss (red-dashed line).

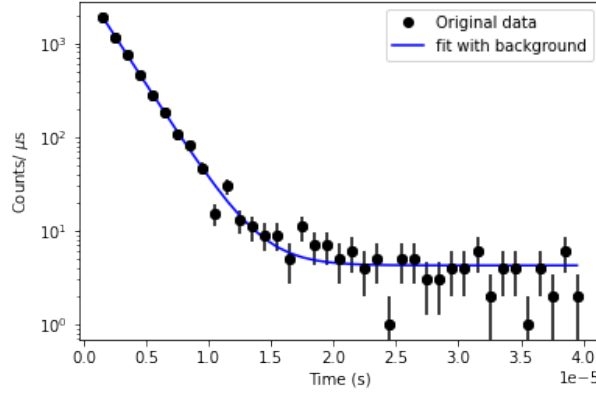


Figure 3: This graph shows the spectrum of measured time intervals between pulses. The smooth curve is an exponential with a constant background.

### 3.3 Muon and Decay Pulse-Height Histograms

Incident muons traveling at near light-speeds that triggered the detector show a distinct pulse-height spectrum as plotted as a function of its energy loss in MeV. In figure 4 we counted each stopped muon by measuring counts per 2.39 MeV with energy losses in MeV on the horizontal. Figure 4 is starkly different than figure 2 due to large discrepancies in the amount of energy being deposited. This is because muons that are able to be stopped have much lower energies than those that pass straight through our detector.

An average energy loss of 47.33 MeV was calculated and used for calibration on our graphs using the dimensions of our detector, the mean stopping power for sea level muons, and the density for muons in sodium-iodide (NaI) [2]. We then observe the following signal spike when a decay positron is detected as seen in figure 5. We indicate the average energy loss as a red-dashed line for reference on figure 5. A complete decay energy loss can be obtained up to 53 MeV. Energy losses that occurred after our maximum allowed decay energy of 53 MeV are assumed to come from accidental muon detections and shouldn't be considered in our decay analysis.

## 4 Discussion

In our data analysis process of muons approaching Earth's atmosphere some approximations were made that could be enhanced with future detectors. In our experiment, 4 GeV muons were assumed to be the average at sea-level incident vertically on our detectors surface after losing energy through ionization and radiative processes [4]. We rely on larger particle observatories to provide ratios of cosmic flux and their relative stopping power energies that were helpful in generating our energy loss calculations. Our experiment was designed to capture muons with low

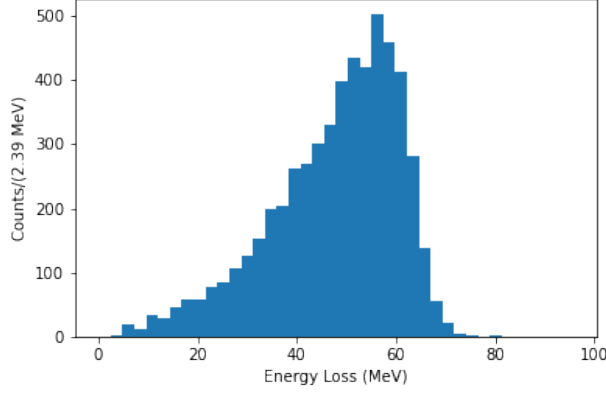


Figure 4: Energy-loss spectrum of the incident low-energy muons that then decayed shortly after detection.

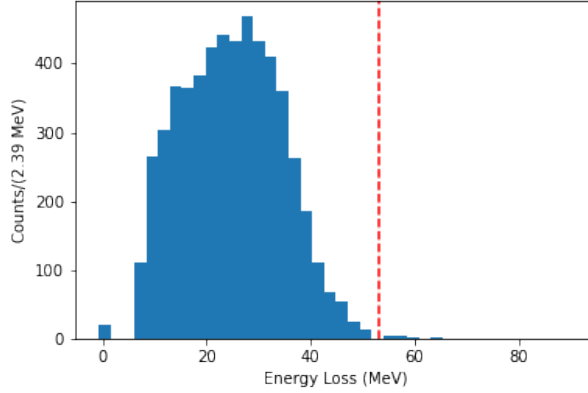


Figure 5: Energy-loss spectrum of the decay particle. The vertical dashed-line represents the maximum energy of the positron/electron emitted in  $\mu^+$  decay.

enough energy that decays could be captured: effectively trapping the muon whilst it decayed. Not all possible decay combinations could be detected. For instance, muons that pass through the detector with higher energies are numerous. And we note that the alternate decay sequence containing an electron was left out of our data due to not interacting with our detector arrangement. Future experiments may look to increase detection capabilities in this regard.

## 5 Summary

Successful detection of low-energy sea-level muon decays were made using our Sodium-Iodide (NaI) detector at the Ursinus Lab. Our results match with expected energies and decay times previously established by professional particle physicists. This experiment may be reproduced with sufficiently high detection rates in time scales starting from as short as a single week worth of data. In our initial experiment we ran our detector for approximately 4 weeks and in that time we detected 5,532 potential decay events and perform a detailed energy and time analysis on incident muon decay processes. This work could be extended to account for the impact of  $\mu^-$  capture on the measured mean  $\mu$  lifetime. Energy-loss calculations showed a spectrum of ranges for low-energy muon capture. This data may be used for enhancing future laboratory analysis in the detection of muons and give a strong introduction into particle detection systems.

## References

- [1] Ulrik Egede, Gösta Gustafson, Christina Zacharatou Jarlskog, and Janus Schmidt-Sørensen. Parity violation in muon decays and the muon lifetime. page 34.
- [2] Striganov N.V. S.I. D.E. Groom, Mokhov. Muon stopping-power and range tables, 10 MeV–100 TeV, 2001.
- [3] Sherman Ip. The Decay of Muons, December 2012.
- [4] K Nakamura et al. Review of Particle Physics, Journal of Physics G: Nuclear and Particle Physics 37, 075021 (2010).
- [5] L.A Riley. udaq command-line/Python interface for data acquisition from a 5000-series PicoScope, 2022.